J Fluoresc (2011) 21:2143–2153
DOI 10.1007/s10895-011-0916-1

ORIGINAL PAPER

Determination of Copper(II) Ion Concentration by Lifetime Measurements of Green Fluorescent Protein

Benjamin Hötzer · Rumen Ivanov · Silke Altmeier · Reinhard Kappl · Gregor Jung

Received: 15 March 2011 / Accepted: 4 July 2011 / Published online: 20 July 2011

Abstract The understanding of cellular processes and functions and the elucidation of their physiological mechanisms is an important aim in the life sciences. One important aspect is the uptake and the release of essential substances as well as their interactions with the cellular environment. As green fluorescent protein (GFP) can be genetically encoded in cells it can be used as an internal sensor giving a deeper insight into biochemical pathways. Here we report that the presence of copper(II) ions leads to a decrease of the fluorescence lifetime (τ_{fl}) of GFP and provide evidence for Förster resonance energy transfer (FRET) as the responsible quenching mechanism. We identify the His_6-tag as the responsible binding site for Cu^{2+} with a dissociation constant $K_d = 9 \pm 2$ μM and a Förster radius $R_0 = 2.1 \pm 0.1$ nm. The extent of the lifetime quenching depends on $[Cu^{2+}]$ which is comprehended by a mathematical titration model. We envision that Cu^{2+} can be quantified noninvasively and in real-time by measuring τ_{fl} of GFP.

Keywords TCSPC · GFP · Biosensor · Fluorescence · Titration

B. Hötzer · S. Altmeier · G. Jung (✉)
Department of Biophysical Chemistry, Saarland University, Campus B2 2, 66123 Saarbrücken, Germany
e-mail: g.jung@mx.uni-saarland.de

R. Ivanov
Department of Biosciences-Plant Biology, Saarland University, Campus A2 4, 66123 Saarbrücken, Germany

R. Kappl
Department of Biophysics, Saarland University, Building 76, 66421 Homburg, Germany

Introduction

Transition metal ions like iron, copper, cobalt and zinc play an essential role in biology and medicine. Heavy metal ions also are of crucial importance in the environmental context [1]. In most cases one specific metal ion performs one or only a few functions. Consequently, distinction between the various metal ions is desirable in bioinorganic chemistry [2].

In particular, the knowledge of $[Cu^{2+}]$ is of utmost interest because Cu^{2+} is an essential micronutrient for all living organisms. Participating as a catalytic cofactor in multiple metabolic pathways due to its redox properties [3, 4], Cu^{2+} is needed within mitochondria for the function of cytochrome oxidase, within the *trans*-Golgi network to supply secreted cuproproteins and within the cytosol to supply superoxide dismutase [5]. Plastocyanin in cyanobacteria, algae and the chloroplasts of plants also requires Cu^{2+} [6, 7]. Furthermore Cu^{2+} is involved in the formation of structural compounds of biomolecules and signaling molecules [8, 9].

The insufficient availability of Cu^{2+} can be deleterious. In humans, Cu^{2+} deficiency causes mitochondria abnormalities and neurodegeneration [10], while in plants, it leads to severe chlorosis affecting crop yields [11]. When present at elevated concentrations, Cu^{2+} triggers the formation of reactive oxygen radicals in eukaryots and prokaryots which damage the intracellular membranes, proteins and nucleic acids [12, 13]. The latter action is presumably the basis of its antibiotic effect [14, 15]. Also the role of Cu^{2+} in ailments like Wilson's disease and Alzheimer's disease deserves further investigations [16, 17]. The range of $[Cu^{2+}]$ which has a beneficial physiological impact is in the micromolar range. The optimal growth of the cells of

the bacterium *M. capsulatus* requires [Cu^{2+}] of about 30 μM, the exchangeable Cu^{2+} pool concentration in blood is about 8 μM [18]. This makes the analysis of the copper homeostasis an important aim [19]. It should be noted that also Cu^{+} as prevalent state of copper ions is under debate. Only the development of selective sensors for this lower oxidation state allows for imaging its appearance [20–22]. Therefore, it is desirable to provide also a selective tool for the quantitation of [Cu^{2+}].

Various methods for the detection of [Cu^{2+}] were previously described. These are for instance the measurement of the fluorescence intensity of quantum dots [23, 24], potentiometric and voltammetric detection [25] just as well as optical sensing due to Schiff base method [26, 27] and an electrochemical approach [28].

Other approaches use fluorescent proteins (FPs). The use of FPs revolutionized the life sciences as a result of their manifold applicabilities and their unique optical and structural properties [29]. Together with the fact that no exogenous substrates and cofactors are required for the generation of fluorescence, the ubiquitious expression of FPs in cells make these proteins a standard tool in biosciences [30]. Owing to the significance of GFP the Nobel prize for Chemistry was awarded to O. Shimomura, M. Chalfie and R. Tsien in 2008 [31]. With respect to the above mentioned quantitation of [Cu^{2+}] levels it was shown, that the fluorescence intensity of DsRed is quenched by Cu^{2+} [32, 33]. Other work previously inserted a heavy metal ion binding site close to the chromophore [34, 35]. For the quantitative determination of the [Cu^{2+}], however, these methods are not suited as the proposed systems are not self-referencing. This means, that the fluorescence intensity strongly depends on the local GFP concentration. A calibration of the copper free system has to be done before the actual measurement. Secondly, we have shown in the past that the fluorescence intensity of several FPs strongly depends on their photophysical properties like dark-state population and on their illumination history [36–38]. We will show, that most of the mentioned problems can be overcome by measuring the fluorescence lifetime (τ_{fl}) of GFP while avoiding response to other heavy metal ions.

In this report, a concept for a [Cu^{2+}] biosensor is introduced. This application of GFP is possible since its τ_{fl} strongly depends on [Cu^{2+}] obeying a titration behavior. We demonstrate that the quenching mechanism is Förster resonance energy transfer (FRET) from GFP to Cu^{2+}. Quenching of τ_{fl} due to the presence of Co^{2+}, Ni^{2+}, Fe^{2+}, Mn^{2+} and Zn^{2+} is not observed. The binding site for Cu^{2+} is proven to be the His_6-tag which is already incorporated for the purification of the protein. For the quantitation of Cu^{2+} over a large concentration range, a mathematical titration expression is developed which yields [Cu^{2+}] from the measured τ_{fl} of GFP. Thus a highly Cu^{2+} selective sensor is feasible. Altogether, we exemplify that the measurement of τ_{fl} of His_6-tagged GFP provides a powerful biosensor for the quantitation of [Cu^{2+}].

Experimental Section

TCSPC

Lifetime values are acquired by a home-built setup. The excitation sources are two fiber coupled pulsed diode lasers emitting at 405 nm (LDH-P-C-405, Picoquant, Germany) and 470 nm (LDH-P-C-470B, Picoquant, Germany). The pulse width for both lasers is about 70 ps. Lasers are driven by an oscillator module (PDL 808-MC *Sepia*, Picoquant, Germany) at a repetition rate of 40 MHz. The parallelized excitation beams are focussed in the cuvette. Fluorescence is collected under magic angle conditions in 90° geometry. The photons are detected by an avalanche photodiode (PDM 100ct, Micro Photon Devices, Italy). The FWHM of the instrument response function (IRF) is about 200 ps. Electronical signals are recorded by a stand-alone time-correlated single photon counting (TCSPC) module (PicoHarp300, Picoquant, Germany). The readout is synchronized by the software (SymPhoTime, Picoquant, Germany). The obtained lifetime values result from mono- resp. biexponential reconvolution fitting (FluoFit, Picoquant, Germany) as described in the text. $\chi^2 < 1.2$ for all measurements except monoexponential reconvolution fits at high [Cu^{2+}] due to the better appropriateness of the biexponential fitting model.

Fluorescent Proteins

Recombinant fluorescent proteins are produced in the *E. coli* expression strain BL21(DE3) under control of the T7 promoter. A 250 ml culture in Luria-Bertani medium is incubated at 37 °C under continuous shaking until the OD_{600} is 0.6–0.8. The expression is induced by adding IPTG at a final concentration of 1 mM. The culture is harvested after 24 h of further shaking at 20 °C. The His_6-tagged proteins are purified on immobilized metal affinity chromatography columns using Ni-NTA resins. SDS gel electrophoresis and Coomassie staining are employed to check the purity of the proteins. The samples are prepared in phosphate-buffered solution at pH 7.4 (NaCl 115 mM, Na_2HPO_4 16 mM,

KH_2PO_4 4 mM). The eYFP has a C-terminal His_6-tag followed by an enterokinase cleavage site (Asp_4Lys). In an aliquot of eYFP, the His_6-tag is removed using Tag-off™rEK Cleavage/Capture Kit (Novagen, Merck KGaA, Darmstadt, Germany) according to the instructions of the manufacturer with an incubation time of 20 h. The His_6-tag peptide is removed from this eYFP solution by repeated immobilized-metal affinity chromatography on His-select®spin columns (Sigma-Aldrich, Saint Louis, MO, USA). The purity of the eYFP without His_6-tag is confirmed by SDS gel electrophoresis and Coomassie staining.

Sample Preparation

Buffered stock solutions of all used GFP variants are diluted with pure water in order to avoid the precipitation of unrequested copper complexes which would effect the actual $[Cu^{2+}]$. [GFP] is always in the submicromolar range. For the titration experiments $Cu(SO_4)\bullet 5H_2O$, $Co(SO_4)\bullet 7H_2O$, $Ni(SO_4)\bullet 7H_2O$, $Fe(SO_4)\bullet 7H_2O$, $Mn(SO_4)\bullet H_2O$ and $Zn(SO_4)\bullet 7H_2O$ are dissolved in distilled water to 1 M stock solutions which are subsequently diluted. Absorption spectra of Cu^{2+}, Co^{2+}, Ni^{2+}, Fe^{2+}, Zn^{2+} and Mn^{2+} are measured with $1 \cdot 10^{-4}$ M metal ion concentration and a $5 \cdot 10^{-4}$ M concentration of poly-l-histidine (Sigma-Aldrich, Saint Louis, MO, USA). Poly-l-histidine is used to simulate the histidine side chains of the His_6-tag.

EPR Spectroscopy

EPR spectra are recorded on an EPR spectrometer (Elexsys 680, Bruker, Germany) equipped with a continuous flow helium cryostat ESR 900 and an ITC 502 temperature controller (Oxford Instruments, England) to allow measurements down to 5 K. Temperature and microwave power are adjusted such that no spectral saturation occurs (20 K, 0.5 mW). Modulation amplitudes of 0.7 or 0.39 mT are used at 100 kHz frequency. The microwave frequency is measured with a frequency counter (HP 5350B, ValueTronics, USA), the magnet field with a NMR-Gaussmeter. Spectra are accumulated to yield an acceptable signal-to-noise ratio. Samples of 150 μl were filled in an EPR quartz tube (Wilmad, USA) and frozen in liquid nitrogen for measurement and storage.

Optical Spectroscopy

Absorption spectra are recorded with a two beam spectrophotometer (Lambda 5, Perkin Elmer, USA). Excitation and emission spectra are measured using a fluorescence spectrometer (FP-6500, Jasco, Germany) in 90° geometry. All spectra are recorded at a resolution of 1 nm.

Mathematical Treatment of the Lifetime Data

Lifetime histograms as shown in Fig. 1 are obtained by TCSPC. As will be explained in section "Results and Discussion" in more detail τ_{fl} always refers to the average lifetime τ_{av} which is derived by monoexponential fitting according to $I(t) = A_{av} \times e^{-\frac{t}{\tau_{av}}}$ (Fig. 1a). This is the most unbiased way to analyse the experimental data. Nevertheless, this is a simplification of the true nature. Regarding the system Cu^{2+}-GFP more closely this procedure is not quite justified at first glance. GFP T203H has a monoexponential lifetime of $\tau_{free} = 3.4$ ns. The addition of Cu^{2+} leads to the formation of a Cu^{2+}-GFP complex with a distinct lifetime of $\tau_{bound} = 1.4$ ns. The mixture of GFP with Cu^{2+} therefore contains species of free GFP and the Cu^{2+}-GFP complex in variable ratios. Hence, exact calculations should be done by biexponential fitting according to $I(t) = A_{free} \times e^{-\frac{t}{\tau_{free}}} + A_{bound} \times e^{-\frac{t}{\tau_{bound}}}$ (Fig. 1b). As already mentioned in the experimental section "TCSPC", a biexponential approach significantly improves the fit at high $[Cu^{2+}]$. This leads to two fixed lifetime values, i.e. τ_{free} and τ_{bound}, and the varying amplitudes A_{free} and A_{bound}, $A_{free} + A_{bound} = 1$. For negligible $[Cu^{2+}]$ $\tau_{av} \approx \tau_{free}$, whereas if all GFP molecules are bound with Cu^{2+}, then $\tau_{av} \approx \tau_{bound}$. A biexponential analysis is compared with the monoexponential approach in Fig. 1. Although in this particular case of high $[Cu^{2+}]$ a biexponential fit is considerably better than usage of only one exponent, this is not true for all $[Cu^{2+}]$.

The connection between the monoexponential lifetime τ_{av} and the biexponential lifetimes τ_{free} and τ_{bound} is given by $\tau_{av} = A_{free} \times \tau_{free} + A_{bound} \times \tau_{bound}$. The total amount of GFP, GFP_{tot}, is given by $[GFP]_{tot} = A_{free} \times [GFP]_{tot} + A_{bound} \times [GFP]_{tot}$. This means $[GFP]_{free} = A_{free} \times [GFP]_{tot}$ and $[GFP]_{bound} = (1 - A_{free}) \times [GFP]_{tot}$. Replacing A_{bound} by $(1 - A_{free})$ leads, after reordering, to

$$A_{bound} = \frac{\tau_{av} - \tau_{free}}{\tau_{bound} - \tau_{free}}. \quad (1)$$

An equation for the intensity titration curve was previously described [39]:

$$[GFP \times Cu] = [Cu]_{tot} \times [GFP]_{tot}/K_d + [Cu]_{tot}. \quad (2)$$

It should be noted that Eq. 2 is only true under the assumption, that the fraction of bound Cu^{2+} is negligible.

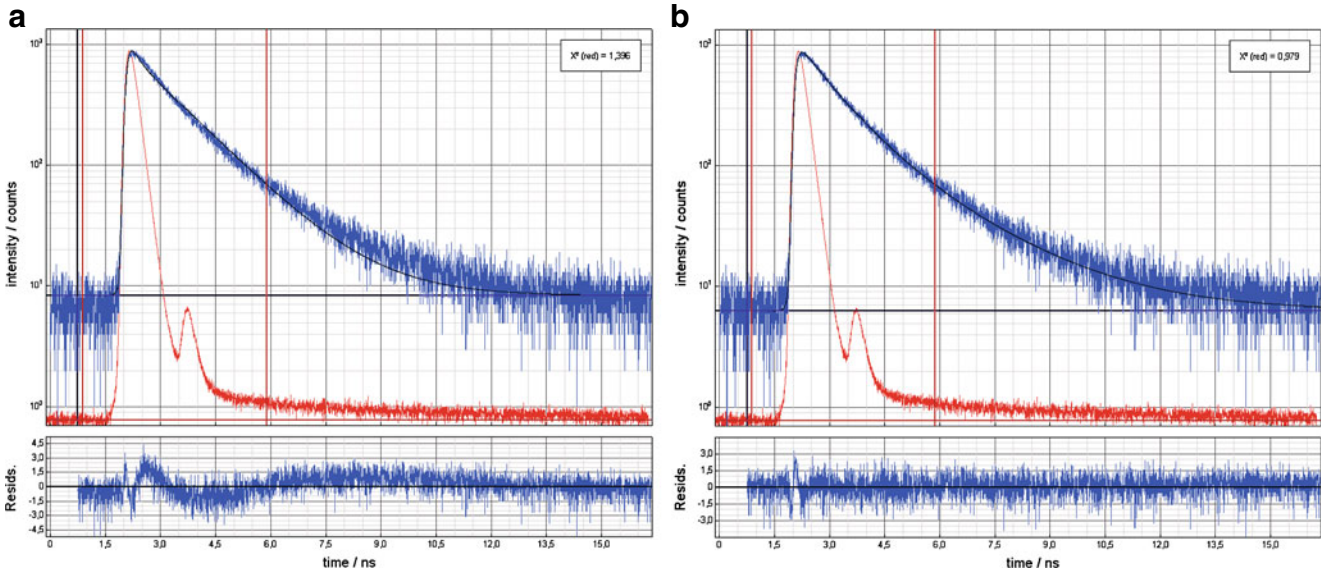

Fig. 1 **a** Lifetime histogram of a submicromolar GFP T203H solution after the addition of 10^{-5} M [Cu^{2+}]. The average lifetime τ_{av} is computed by a monoexponential fit. **b** Analysis of the same measurement as in Fig. 1a by a biexponential fit. Inspection of the fit residuals clearly favors a biexponential model. However, the biexponential fit does not considerably improve the fit residuals at lower [Cu^{2+}]

Bearing in mind that A_{bound} in Eq. 1 corresponds to $[GFP-Cu]/[GFP]_{\text{tot}}$, inserting Eq. 1 in the intensity formula, Eq. 2, yields Eq. 3. This equation is used for the evaluation of the τ_{fl} titration when τ_{av} is replaced by τ_{fl}.

$$\tau_{\text{fl}} = \tau_{\text{bound}} + \frac{(\tau_{\text{free}} - \tau_{\text{bound}}) \times [Cu^{2+}]}{[Cu^{2+}] + K_d} \tag{3}$$

In Eq. 3 τ_{free} is the value of the unquenched lifetime of the GFP mutant, i.e. 3.4 ns, τ_{bound} is the lifetime of the GFP mutant after the formation of the Cu^{2+}-GFP complex, i.e. 1.4 ns.

Hence all lifetime calculations can be done either by monoexponential or by biexponential fitting. Fitting according to the monoexponential model has the advantage of being better transferable to low absolute count events like they occur while performing FLIM. Especially in these experiments where global fitting due to a lack of concentration steps is not possible, results that stem from the monoexponential decay model are more straightforward and interpretable than such from the biexponential decay model. We make use of τ_{av} in phenomenological investigations in section "Phenomenological Fitting". Here, simulations of the lifetime characteristics are done preferentially by using τ_{av} because formula (3) describes lifetime titrations and can be easily modified for other titration models. Nevertheless, for fluorescence lifetime titration experiments the biexponential model is more consistent with the true conditions on the molecular level.

Results and Discussion

Effect of Copper on the GFP Lifetime

In the past, a heavy metal ion binding site was introduced close to the chromophores in YFPs. This binding site was sensitive to a large variety of transition metal ions like copper, nickel, zinc etc. [35]. We expect that already the His_6-tag of proteins which is incorporated for affinity chromatography can bind heavy metal ions in a useful way and thus quench the fluorescence [40, 41]. We reason that not only the fluorescence intensity but also τ_{fl} can be exploited for analytical purposes. To prove this, we add Cu^{2+} to a solution of GFP mutant T203H with His_6-tag. This leads to a decrease of the fluorescence intensity as well as to a reduction of τ_{fl} (Fig. 2a). The extent of the τ_{fl} quenching of GFP depends on [Cu^{2+}]. Higher concentrations of Cu^{2+} lead to a more distinct reduction from the initial value of $\tau_{\text{fl}} = 3.4$ ns of the unquenched GFP. The concentration dependent quenching of τ_{fl} makes GFP a suitable tool to determine [Cu^{2+}] by means of lifetime measurements. Figure 2b shows the titration curve of τ_{fl} of GFP with Cu^{2+} where Eq. 3 describes the curve progression.

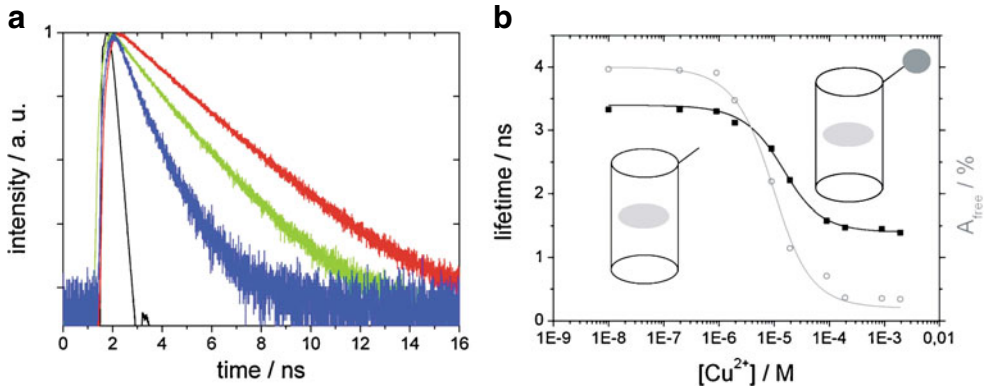

Fig. 2 **a** Decrease of $\tau_{fl} = 3.4$ ns of GFP mutant T203H (*red*) in a concentration of 5.0×10^{-7} M due to the addition of Cu^{2+}. The *green curve* corresponds to $\tau_{fl} = 2.5$ ns at $[Cu^{2+}] = 5.0 \times 10^{-6}$ M, the *blue curve* to $\tau_{fl} = 1.4$ ns where $[Cu^{2+}]$ is 2.5×10^{-3} M. The IRF ($\lambda_{ex} = 405$ nm) is shown in *black*. **b** Comparison of the titration results by monoexponential fitting (*black squares*) with biexponential fitting (*grey open symbols*) of the fluorescence lifetime of the same GFP T203H sample. The dissociation constants are $K_d = 1.1 \times 10^{-5}$ M for the monoexponential fit and $K_d' = 7 \times 10^{-6}$ M for the biexponential fit which is in good agreement within the errors

The dissociation constant is given by K_d. From a fit to the data points, $K_d = 11 \pm 2 \times 10^{-6}$ M is obtained. A biexponential fit, in which the coexistence of a quenched ($\tau_{bound} = 1.4$ ns) and an unquenched fluorophor ($\tau_{free} = 3.4$ ns) is taken into account, yields a slightly smaller value ($K_d = 7 \pm 2 \times 10^{-6}$ M). We take $K_d = 9 \pm 2 \times 10^{-6}$ M as the average of both values.

Binding Between GFP and Copper

A matter of interest is the binding site which is sensitive for Cu^{2+}. As histidine is known to bind heavy metal ions we presume the formation of a complex between GFP and Cu^{2+} [42]. Therefore, we suggest the His_6-tag at the C-terminus of the GFP molecules as binding site for Cu^{2+} [43, 44]. For DsRed, however, evidence was provided that this protein has a natural Cu^{2+} binding site [33, 45]. We therefore have to exclude the possibility of the formation of such complexes.

To confirm the formation of a Cu^{2+} histidine complex we enzymatically cleave off the His_6-tag of eYFP. The use of eYFP instead of GFP T203H is mandatory because the cleavage site for the His_6-tag is only present in eYFP but not in our GFP mutant T203H. Quenching of τ_{fl} due to Cu^{2+} occurs for untreated eYFP as well as for GFP T203H. This finding strongly indicates a common behavior which is expected due to the similar spectral properties. Two samples of eYFP in equal concentrations of 5.0×10^{-7} M are prepared whereof one contains eYFP with His_6-tag and the other eYFP lacking the His_6-tag. Lifetime titration measurements as a function of $[Cu^{2+}]$ are done for both samples (Fig. 3a). For the eYFP without His_6-tag the quenching occurs at significantly higher $[Cu^{2+}]$ than for eYFP with His_6-tag. This implies the formation of a Cu^{2+}-GFP complex via the His_6-tag of the GFP. It also implies that the formation of the complex is the reason for the lifetime decrease due to Cu^{2+}. It should be noted, that the intrinsic τ_{fl} of the His_6-tagged protein is restored upon addition of strongly chelating agents like imidazole (data not shown). That fluorescence quenching of eYFP without His_6-tag still appears at high concentrations is not expected at first glance. This effect might result from the binding of Cu^{2+} at other places at the eYFP molecule with lower binding constants e.g. different amino groups [46].

Next, we perform EPR experiments at cryogenic temperatures in order to further characterize the binding coordination of Cu^{2+}. Cu^{2+}-EDTA (5×10^{-4} M) in a glassy ethylene glycol matrix is used as a reference, Fig. 3b. Two samples of eYFP, with His_6-tag, are prepared in an approximately 1:1 stoichiometry in two different concentrations, i.e. $[eYFP]_{low} = [Cu^{2+}]_{low} = 2 \times 10^{-5}$ M and $[eYFP]_{high} = [Cu^{2+}]_{high} = 1 \times 10^{-4}$ M. At $g_\perp = 2.052$ the more diluted sample shows a modulation of the signal due to a hyperfine coupling. Because 6 lines with a splitting of about 1.5 mT are clearly resolved, we attribute these lines to the interaction of at least 2 or 3 equivalent nitrogens with the copper ion. Due to the nuclear spin of I = 1 for ^{14}N, for three coordinating nitrogens seven lines are expected ($2n \times I + 1$, $n = 3$) for which typical hyperfine values around $A_N = 1.5$ mT are found for some copper proteins and copper model complexes [47, 48]. Along the parallel spectral component ($g_\parallel = 2.251$) no indication of nitrogen interactions are observed on the three broad resolved

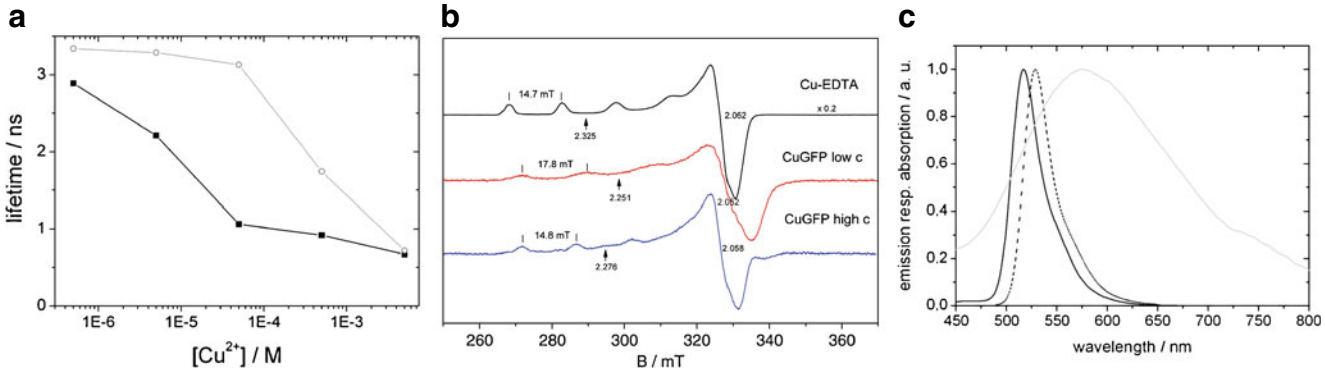

Fig. 3 **a** Fluorescence lifetime titration of eYFP with (*black squares*) and without (*grey open symbols*) His_6-tag. Quenching for eYFP without His_6-tag occurs at about 100-fold higher concentrations compared to eYFP with His_6-tag. This observation supports the formation of a complex between Cu^{2+} and GFP via the His_6-tag. **b** EPR spectra of Cu^{2+}-GFP at concentrations of 2×10^{-5} M (low c) and 1×10^{-4} M (high c) in comparison to the reference sample Cu^{2+}-EDTA in a glassy matrix. The apparent values of the g-tensor are given for the parallel (*arrows*) and perpendicular components, as well as the Cu-hyperfine coupling of the parallel component. Cu^{2+}-GFP in low concentration (low c) shows a barely resolved hyperfine pattern of six lines on top of the perpendicular signal component (2.052). **c** Spectral overlap of the donor emission spectrum of GFP T203H (*black*, $\lambda_{ex} = 405$ nm) and eYFP (dotted) with the absorption spectrum of a Cu^{2+} polyhistidine complex (*grey*). The maximum $\epsilon_{acc}(\lambda_{max} = 575\text{nm})$ is 112 $M^{-1}cm^{-1}$. The width of the acceptor spectrum of ~ 200 nm is beneficial for a large $J(\lambda)$ and for the insensitivity of the spectral behavior of the donor

Cu (I = 3/2) hyperfine lines with the characteristic large couplings $A_\parallel = 17.8$ mT. The higher concentrated sample more closely resembles the Cu-EDTA-sample with respect to the copper hyperfine coupling ($A_\parallel = 14.8$ mT) and the general shape of the perpendicular spectral feature ($g_\perp = 2.058$) without a resolved nitrogen coupling. Copper proteins and model compounds can be classified with respect to their coordination by plotting $A_\parallel$ (in cm^{-1}) vs. $g_\parallel$ yielding distinct regions for S_4, N_4 or O_4 coordination [49]. In such a representation both eYFP samples are located close to N_4-locations whereas the Cu-EDTA sample is in between N_4 and O_4 coordination. Moreover, the ratio $g_\parallel/A_\parallel$ is used as an empirical index for the tetrahedral deviation from a square-planar configuration ranging from 105 to 135 cm for square-planar up to 250 cm for slight and to 700 cm for strong tetrahedral distortions. In this context, the low concentration sample with a ratio of 135 cm is associated with a square planar arrangement whereas the higher concentrated sample and Cu-EDTA (ratios 165, 169 cm) show a small deviation from planarity.

We can summarize that the EPR experiments hint at a binding geometry with at least two but, most likely, four nitrogen atoms forming an almost quadratic-planar complex; different samples, however, display variable coordination geometries indicative for some structural heterogeneity of the possible binding sites. Recent simulations showed that Cu^{2+} is coordinated in a His_6-tag by two, non-neighboring histidines thus supporting our analysis [50, 51].

Also, the extracted K_d (Fig. 2b) is in the range of typical values for binding metal ions to a His_6-tag [52]. Moreover, the consideration of two binding sites following the model for polyprotic acids [53] is not compatible with our experimental data, see below in Fig. 4b.

Phenomenological Fitting

To gain a deeper understanding of the binding characteristics between Cu^{2+} and the His_6-tag the titration curve is fitted by a modified equation. Equation 3 can be extended by the Hill factor n that modifies the slope of the curve in dependence of the binding. This leads to Eq. 4.

$$\tau_{fl} = \tau_{bound} + \frac{(\tau_{free} - \tau_{bound}) \times [Cu^{2+}]^n}{[Cu^{2+}]^n + K_d^n} \quad (4)$$

For $n = 0.5$, 1.0, 2.0 and 3.0 fits are performed for the experimentally derived titration curve. The results are shown in Fig. 4a. For $n = 1$ the titration curve represents the result from Fig. 2b according to Eq. 3.

The behavior for $n = 1$ which corresponds to an independent binding of Cu^{2+} to the His_6-tag nicely matches the experimentally derived values. For $n < 1$, i.e. 0.5, binding of a molecule inhibits the binding of further molecules. This leads to a decreased slope. Regarding $n > 1$, i.e. 2.0 and 3.0, the slope is increased. Like shown in Fig. 4a these curve shapes do not represent

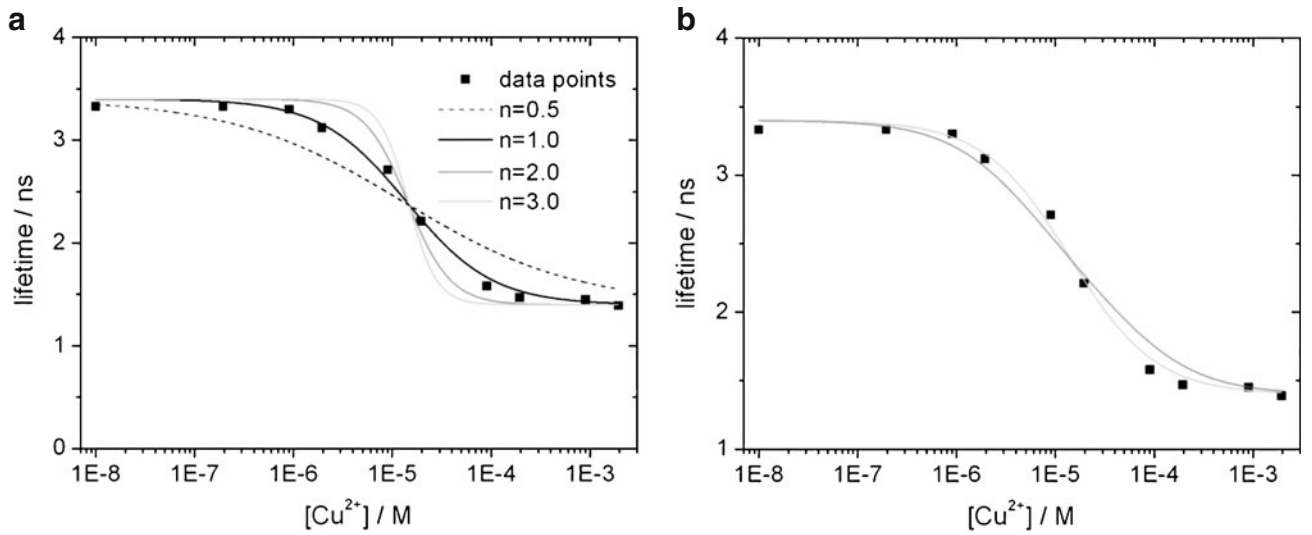

Fig. 4 **a** Titration curve of the fluorescence lifetime of GFP mutant T203H (*black squares*). The trend is fitted according to Eq. 4 for $n = 0.5$, 1.0, 2.0 and 3.0. **b** Titration curve of the fluorescence lifetime of GFP mutant T203H (*black squares*). The figure shows the models for one titration step (*light gray*) and for two titration steps (*dark gray*)

the experimentally observed curve progressions. These results suggest that the binding of Cu^{2+} to the His_6-tag is independent of already bound copper ions, i.e. there is no cooperativity in the Cu^{2+} binding.

To further investigate the possible binding of two Cu^{2+} to the His_6-tag the model is extended by a second titration step with different K_d values. This two-site binding approach is based on the linear combination of titration curves for individual binding sites [53] and leads to Eq. 5.

$$\tau_{fl} = \tau_1 + \frac{(\tau_3 - \tau_2) \times [Cu^{2+}]}{[Cu^{2+}] + K_1} + \frac{(\tau_2 - \tau_1) \times [Cu^{2+}]}{[Cu^{2+}] + K_2} \quad (5)$$

Figure 4b shows the titration curve of τ by Cu^{2+} fitted with the one titration step model and simulated by the two-site binding model. The simulation is done for $\tau_1 = 3.4$ ns, $\tau_2 = 2.3$ ns and $\tau_3 = 1.4$ ns with K_d values $K_1 = 5 \cdot 10^{-5}$ M resp. $K_2 = 5 \cdot 10^{-4}$ M according to Eq. 5.

On the basis of the comparison we cannot find any convincing evidence for the binding of two Cu^{2+} ions. We therefore conclude that the formation of a His_6-tagged GFP, complexed with only one Cu^{2+} via ≥ 2 His, is responsible for the change in τ_{fl} of GFP. Yet, the quenching mechanism still has to be clarified.

Possible Quenching Mechanisms

There are several generally possible quenching mechanisms which should be shortly discussed. Static quenching in a conventional sense leads to a decrease of the fluorescence intensity but the fluorescence lifetime is not affected. The reason is, that the non-fluorescent complexes do not contribute to lifetime measurements [54]. Since in the case of GFP and Cu^{2+} a significant change in the lifetime is observed static quenching in its puristical sense can be excluded as cause for the change of τ_{fl}.

Dynamic quenching, in principle, reduces the fluorescence intensity as well as τ_{fl} [55]. Precondition for effective dynamic quenching is a collision between the fluorophor and the quencher during the excited-state lifetime. τ_{fl} in our experiment is in the range of the residence time of two molecules in a common solvent cage. This means, that if the quenching complex is not preformed, then no quenching takes place. The short τ_{fl} therefore excludes dynamic quenching. A Stern–Volmer-plot (data not shown) confirms this argumentation.

Photoinduced electron transfer (PET) as a molecular mechanism occurs for distances < 1 nm [56]. Considering the geometrical structure of GFP, the distance between the His_6-tag bound Cu^{2+} and the GFP chromophore is larger than two nanometers. This means that PET cannot be responsible for the drop of the lifetime. Long-range electron transfer which is observed in DNA [57] is also discussed for flexible peptides [58, 59]. However, the aqueous environment to which at least the His_6-tag is exposed, as well as the conformational stiffness of GFP makes an electron hopping in the present case unlikely. Also the absence of any distinct

effect for other redox active ions (see below) alludes to another quenching mechanism.

FRET Leads to a Change in the Lifetime

Excluding all other mechanisms, we suspect FRET as the quenching mechanism. FRET describes the phenomenon of non-radiative energy transfer from an electronically excited donor to an acceptor in the ground state. Precondition for FRET is a spectral overlap of the emission spectrum of the donor with the absorption spectrum of the acceptor. FRET is a strongly distance dependent process which occurs in a range of about 1–10 nm [60]. In order to investigate this possibility, we record absorption spectra of the putative FRET acceptor Cu^{2+}. Upon addition of Cu^{2+} to a solution of polyhistidine a blue color of the sample appears (Fig. 3c) due to the formation of a copper-histidine complex [61]. Polyhistidine is chosen as a substitute for the His_6-tag, simulating the side chains of the latter thus allowing for examining the optical properties of the Cu^{2+} complex with GFP. We conclude that a similar blue complex due to the binding of Cu^{2+} to the His_6-tag is formed. The low optical extinction of the complex ($\epsilon_{acc} = 112\ M^{-1}cm^{-1}$ at $\lambda_{max} = 575$ nm), which is in good agreement with previous results [61], prevents us from measuring the effect directly on GFP. The green fluorescence of GFP and the absorption of the Cu^{2+} complex indicate good spectral overlap $J(\lambda)$ (Fig. 3c) which is a prerequisite for FRET. Slight spectral shifts of the spectra as observed for e.g. eYFP do not influence $J(\lambda)$ significantly and therefore result in similar R_0. The fact that FRET is a purely photophysical effect explains why the fluorescence quenching could also be verified for several other GFP mutants including S65T which all possess a His_6-tag.

The question whether FRET really occurs can be answered by calculating the Förster radius R_0 on the basis of the spectral overlap integral $J(\lambda)$. Energy transfer in any donor-acceptor pair is specified according to Eq. 6 [62]:

$$R_0^6 = \frac{9000 \times \ln(10) \times \kappa^2 \times Q_D}{128 \times \pi^5 \times N_A \times n_0^4} \times \underbrace{\int_0^\infty F_D(\lambda) \times \epsilon_{acc}(\lambda) \times \lambda^4 d\lambda}_{J(\lambda)} \quad (6)$$

The orientation factor κ^2 describes the relativ orientation of the transition dipoles of the donor and the acceptor. Each GFP molecule has one His_6-tag at the C-terminus as binding site for Cu^{2+}. The flexibility of the His_6-tag enables the rotation of the Cu^{2+} histidine complex with respect to the GFP molecule. We therefore assume $\kappa^2 = 2/3$ owing to dynamic random averaging [63]. It should be noted that the dipole approximation might be invalid for Cu^{2+} as acceptor because hydrated Cu^{2+}-ions do not exhibit significant polarization effects in absorption [64]. However, as the transition dipole moment of the GFP chromophore is perpendicular to the connection line to the absorber in a rough estimation, κ^2 cannot exceed one. Thus, the averaged value $\kappa^2 = 2/3$ should be a good approximation. Similar considerations were made for lanthanides as FRET donors [65]. A quantum yield for a GFP mutant containing T203H of QD = 0.78 [66] and a refractive index of $n_0 = 1.4$ for proteins in aqueous solutions [55] are inserted. N_A describes the Avogadro's number. We obtain $R_0 = 2.1 \pm 0.1$ nm for the pair GFP and Cu^{2+} resp. $R_0 = 2.2 \pm 0.1$ nm for the pair eYFP and Cu^{2+}. This value is only about 40% of R_0 of good donor-acceptor pairs despite a more than 1000-fold smaller extinction ϵ_{acc} in comparison to ϵ_{acc} of conventional organic dyes. In contrast to a rough estimate of the reduction of R_0 on this basis, i.e. $\sqrt[6]{1000} \approx 3$, the diminishing of the spectral overlap is partially compensated due to the broad absorption of the Cu^{2+} histidine complex enhancing the energy transfer. Please note that acceptors with small extinction coefficients are convenient to access smaller Förster radii in photophysical research [67, 68]. Although κ^2 might be misestimated to some extend, R_0 should only be slightly influenced due to the one-sixth power dependence in Eq. 6. Taking into account the obtained R_0 we now calculate the lifetime τ_{bound} of the Cu^{2+}-GFP complex using Eq. 7 [55].

$$E = \frac{R_0^6}{R_0^6 + R^6} = 1 - \frac{\tau_{bound}}{\tau_{free}} \quad (7)$$

For computing τ_{bound} we resort to the dimensions of the GFP molecule. The chromophore consists of three amino acids buried in the center of the protein. The protein exhibits a barrel-like structure of approximately 4.2 nm in height and 2.4 nm in diameter [69]. The flexibility of the His_6-tag enables the rotation of the Cu^{2+}-GFP complex. Ignoring at first the His_6-tag, the distance between Cu^{2+} and the GFP chromophore should be between $1/2 \times 4.2$ nm = 2.1 nm (center) and $\sqrt{2.1^2 + 1.2^2}$ nm = 2.4 nm (edge). For R = 2.1 nm according to Eq. 7 and $R_0 = 2.1$ nm we receive a FRET efficiency $E = 0.50$. This results in a theoretical value of $\tau_{bound} = 1.7$ ns which matches the experimentally obtained value of $\tau_{bound} = 1.4$ ns. The most likely reason why the estimate does not perfectly coincide with the experimental data is that the assumed position of

Table 1 Förster radii of the metal ion complexes of Cu^{2+}, Co^{2+} and Ni^{2+} with polyhistidine and the two GFP mutants T203H and eYFP

	Cu^{2+}		Co^{2+}		Ni^{2+}	
	T203H	eYFP	T203H	eYFP	T203H	eYFP
$\epsilon_{max}/M^{-1}cm^{-1}$	112		52		23	
λ_{max}/nm	575		509		657	
R_0/nm	2.1	2.2	1.8	1.8	1.4	1.5

the His_6-tag is not fixed but fluctuating on a timescale below τ_{fl}. An averaged dimension of 0.4 nm of the His_6-tag was calculated [51] and a consecutive shortening or extension of the donor-acceptor distance by this value would alter the calculated FRET efficiency by ± 20 % and, likewise, τ_{fl}. Therefore, our experimental results are in good agreement with the dimensions of the protein. Thus, all our calculations support FRET between the His_6-bound Cu^{2+} and the chromophore (Table 1).

Specificity of GFP to Copper(II) Ions

This work is the first step towards the development of a biosensor for Cu^{2+}. Therefore the quenching of τ_{fl} of GFP by other biological relevant metal ions like nickel, iron and cobalt has to be excluded. Especially strongly colored metal ions which are known for absorption in the visible range have to be taken into account since they are possible candidates as FRET acceptors. The extinction coefficients of metal ion solutions of Co^{2+} and Ni^{2+} after the addition of a 3-fold excess of polyhistidine are measured like in the case of Cu^{2+}. The extinction coefficients in the absorption maximum are $\epsilon_{acc} = 52\ M^{-1}\ cm^{-1}$ for Co^{2+} ($\lambda_{max} = 509$ nm) and $\epsilon_{acc} = 23\ M^{-1}\ cm^{-1}$ for Ni^{2+} ($\lambda_{max} = 657$ nm).

Calculating R_0 for GFP T203H and Co^{2+} results in $R_0 = 1.8 \pm 0.1$ nm resp. $R_0 = 1.4 \pm 0.1$ nm for GFP T203H and Ni^{2+}. Since the distance between the binding site and the chromophore is larger than the respective R_0, the effect of the lifetime quenching should not be as pronounced as in the case of Cu^{2+}. In addition, the influence of these ions on the lifetime of GFP is also experimentally examined. The addition of a 10 mM solution of Ni^{2+} reduces τ_{fl} of GFP T203H from 3.4 ns to 3.2 ns. Co^{2+} in a concentration of 10 mM leads to a decrease of τ_{fl} to a value of 2.8 ns (Fig. 5b). The influence of Fe^{2+}, Zn^{2+} and Mn^{2+} is also investigated. The addition of 10 mM solution of these ions does not effect the lifetime of GFP T203H. This result comes up to our expectations as the complexes of these metal ions are colorless in the visible spectral range (Fig. 5a). From these results we conclude that distinct FRET can only happen for Cu^{2+} among the physiologically relevant ions. As expected, only the addition of Cu^{2+} to a solution of GFP leads to a decrease of τ_{fl} as well as of the fluorescence intensity. The specific lifetime change enables the development of a Cu^{2+} biosensor.

Application on Other GFP Mutants

Having excluded the cross-sensitivity of various other metal ions, the approach is investigated for the applica-

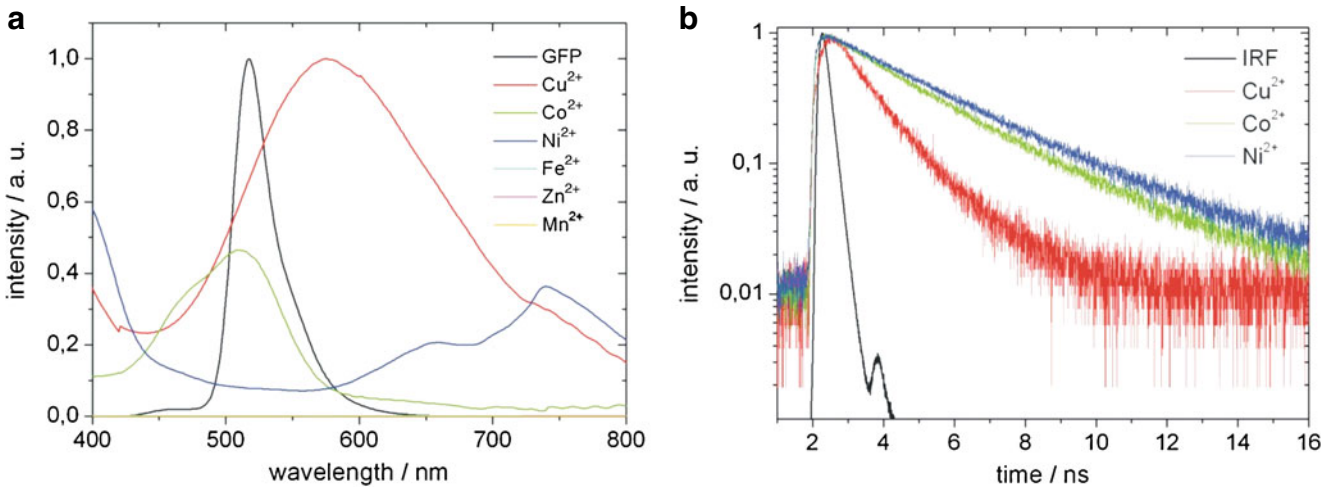

Fig. 5 **a** Emission spectrum of GFP mutant T203H and absorption spectra of polyhistidine complexes with Cu^{2+}, Co^{2+}, Ni^{2+}, Fe^{2+}, Zn^{2+} and Mn^{2+}. The absorption spectra are normalized to the absorption of Cu^{2+}. **b** Decrease of $\tau_{fl} = 3.4$ ns of GFP mutant T203H in a concentration of 5.0×10^{-7} M due to the addition of Cu^{2+}, Co^{2+} and Ni^{2+}. The red curve corresponds to $[Cu^{2+}] = 1.0 \times 10^{-3}$ M, the green curve to $[Co^{2+}] = 1.0 \times 10^{-2}$ M and the blue curve to $[Ni^{2+}] = 1.0 \times 10^{-2}$ M. The IRF ($\lambda_{ex} = 405$ nm) is shown in black

Table 2 Overview over R_0, K_d, τ and E of the investigated mutants of GFP

Mutant	T203H	T203V	eYFP	S65T
R_0 / nm	2.1	2.1	2.2	2.1
K_d / μM	9	2	3	11
τ_{free} / ns	3.4	3.1	2.7	2.7
τ_{bound} / ns	1.4	1.0	1.5	1.2
E	0.59	0.68	0.44	0.56

The good consistence in R_0 is based on the similar optical properties of these mutants which are relevant for the lifetime reduction due to FRET

tion of other GFP mutants. As FRET is the responsible quenching mechanism for the decrease of the lifetime also variants with similar optical properties that possess a His_6-tag should quench τ_{fl}. In order to confirm this, samples of the GFP variants T203V, eYFP, and S65T are prepared and titration curves of τ_{fl} by Cu^{2+} are recorded. Table 2 shows the calculated R_0, the lifetime values of the samples before and after the addition of Cu^{2+}, the FRET efficiency E and the respective K_d.

It turns out that for all investigated GFP mutants all the Förster radii are in the range of 2.1–2.2 nm. This is not unexpected due to the similarity of their emission spectra (data not shown). The deviations of the efficiencies E might be due to slight geometrical alterations which affect E as stated above by its sixth power. Small differences are observed for the K_d values of the GFP variants. This finding might again, result from their varying geometrical properties within the molecule. Summing up these results the construction of a Cu^{2+} sensor on the basis of changes in τ_{fl} of GFP is possible for all mutants that contain a His_6-tag and emit in the broad absorption band of Cu^{2+}, but a calibration has to be performed for each variant before the measurement.

Conclusion

In the present paper, we quantitatively characterized the binding of Cu^{2+} to the His_6-tag of various GFP variants. The shortening of τ_{fl} of His_6-tagged GFP due to the binding of Cu^{2+} was analyzed. The blue color of the Cu^{2+} polyhistidine complex, where polyhistidine was used to simulate the vicinity of the His_6-tag, explains the selectivity over other heavy metal ions. Therefore any formed Cu^{2+} FP complex can act as an acceptor in FRET. FRET as quenching mechanism leads to a Förster radius $R_0 = 2.1 \pm 0.1$ nm. The corresponding energy transfer efficiency E nicely fits to the dimension of the protein. Consequently, $[Cu^{2+}]$ can be selectively measured by fluorescence lifetime measurements when the GFP concentration can be neglected. Although the presented data were merely recorded with GFP mutant T203H, all investigated FPs with a His_6-tag exhibited the same behavior due to the similar spectral properties.

Our experiments provide evidence, that His_6-tagged FPs as selective Cu^{2+} biosensors possess considerable advantages over other existing approaches. The lifetime based model is self-referencing, i.e. independent of the GFP concentration and varying intensity conditions. Population of dark states, photobleaching and other detrimental effects of irradiation do not influence the outcome of the experiments. This makes our approach superior to other methods.

It should be noted, that the actual quantitation of $[Cu^{2+}]$ relies on the precondition of $[GFP] < K_d$. Moreover, interference with other heavy metal ions or varying pH values was not considered in our mathematical treatment. Indeed, competition of more abundant transition metal ions like Zn^{2+} and Mn^{2+} might aggravate quantitation in vivo. We are currently investigating these effects.

In summary, our work describes the development of a selective and universal biosensor for Cu^{2+} which allows for the quantitation of the latter by TCSPC of any fluorescent protein.

Acknowledgements We are indebted to D. Auerbach for help with the expression and N. Baltes for careful reading of the manuscript. The authors also thank T. Seidel (Bielefeld) for kindly providing us with the eYFP-plasmid. This work was supported by German Research Foundation (DFG, grant JU 650/2-1 and 2-2).

References

1. Nriagu J (1979) Copper in the environment, part 1. Wiley
2. Ma Z, Jacobsen FE, Giedroc DP (2009) Chem Rev 109:4644–4681
3. Kao WC, Chen YR, Yi EC, Lee H, Tian Q, Wu KM, Tsai SF, Yu SS-F, Chen YJ, Aebersold R, Chan SI (2004) J Biol Chem 279:51554–51560
4. Schmauder R, Librizzi F, Canters GW, Schmidt T, Aartsma TJ (2005) ChemPhysChem 6:1381–1386
5. Robinson NJ, Winge DR (2010) Annu Rev Biochem 79:537–562
6. Penfield KW, Gerwith A, Solomon EI (1985) J Am Chem Soc 107:4519–4529
7. Peers G, Price NM (2006) Nature 441:341–344
8. Nies DH (1999) Appl Microbiol Biotechnol 51:730–750
9. Lippard SJ, Berg JM (1994) Principles of bioinorganic chemistry. University Science Books, Mill Valley, CA
10. Rossi L, Lombardo MF, Ciriolo MR (2004) Neurochem Res 29:493–504
11. Epstein E, Bloom AJ (2004) Mineral nutrition of plants: principles & perspectives, 2nd edn. Sinauer Associates, Inc
12. Balamurugan K, Schaffner W (2006) Biochim Biophys Acta 1763:737–746

13. Halliwell B, Gutteridge JM (1984) Biochem J 219:1–14
14. Borkow G, Gabbay J (2004) FASEB J 18:1728–1730
15. Michels HT, Moran W, Michel J (2008) Adv Mater Process 166:57–58
16. Ala A, Walker AP, Ashkan K, Dooley JS, Schilsky ML (2007) The Lancet 369:397–408
17. Sarell CJ, Syme CD, Rigby SEJ, Viles JH (2009) Biochem 48:4388–4402
18. Kramer ML, Kratzin HD, Schmitt B, Römer A, Windl O, Liemann S, Hornemann S, Kretzschmar H (2001) J Biol Chem 276:16711–16719
19. Peña MMO, Lee J, Thiele DJ (1999) J Nutr 129:1251–1260
20. Wegner SV, Arslan H, Sunbul M, Yin J, He CJ (2010) Am Chem Soc 132:2567–2569
21. Zeng L, Miller EW, Pralle A, Isacoff EY, Chang CJ (2006) J Am Chem Soc 2006 128:10–11
22. Yang L, McRae R, Henary MM, Patel R, Lai B, Vogt S, Fahrni CJ (2005) Proc Natl Acad Sci USA 102:11179–11184
23. Koneswaran M, Narayanaswamy R (2009) Sens Actuators B Chem 139:104–109
24. Lai S, Chang X, Fu C (2009) Microchim Acta 165:39–44
25. Zanganeh A, Amini M (2009) Sens Actuators B Chem 135:358–365
26. Aksuner N, Hendren E, Yilmaz I, Cukurovali A (2008) Sens Actuators B Chem 134:510-515
27. Yildirim M, Kaya JJ (2010) Fluoresc 20:771–777
28. Xu GR, Yuan Y, Kim S, Lee JJ (2008) Electroanalysis 20:1690–1695
29. Ormö M, Cubitt AB, Kallio K, Gross LA, Tsien RY, Remington SJ (1996) Science 273:1392–1395
30. Chalfie M, Tu Y, Euskirchen G, Ward WW, Prasher DC (1994) Science 263:802–805
31. Ehrenberg M (2008) Scientific background on the nobel prize in chemistry 2008. The green fluorescent protein: discovery, expression and development
32. Eli P, Chakrabartty A (2006) Protein Sci 15:2442–2447
33. Rahimi Y, Goulding A, Shrestha S, Mirpuri S, Deo SK (2008) Biochem Biophys Res Commun 370:57–61
34. Tansila N, Becker K, Na-Ayudhya CI, Prachayasittikul V, Bülow L (2008) Biotechnol Lett 30:1391–1396
35. Richmond TA, Takahashi TT, Shimkhada R, Bernsdorf J (2000) Biochem Biophys Res Commun 268:462–465
36. Jung G, Wiehler J, Zumbusch A (2005) Biophys J 88:1932–1947
37. Jung G, Zumbusch A (2006) Microsc Res Tech 69:175–185
38. Jung G, Werner M, Schneider M (2008) ChemPhysChem 9:1867–1874
39. Voss S, Skerra A (1997) Protein Eng 10:975–982
40. Isarankura-Na-Ayndhyn C, Tantimongcolwat T, Galla H, Prachayansittihad V (2010) Biol Trace Elem Res 134:352–363
41. Guignet EG, Hovius R, Vogel H (2004) Nat Biotechnol 22:440–444
42. Baute D, Arieli D, Neese F, Zimmermann H, Weckhuysen BM, Goldfarb D (2004) J Am Chem Soc 126:11733–11745
43. El Khouri Y, Hellwig P (2009) J Biol Inorg Chem 14:23–34
44. Mesu JG, Visser T, Soulimani F, van Faassen EE, de Peinder P, Beale AM, Weckhuysen BM (2006) Inorg Chem Chem 45:1960–1971
45. Sumner JP, Westerberg NM, Stoddard AK, Hurst TK, Cramer M, Thompson RB, Fierke CA, Kopelman R (2006) Biosens (2006) Biosens Bioelectron 21:1302–1308
46. Wilson EW, Kasperian MH, Martin RB (1970) J Am Chem Soc 92:5365–5372
47. Hund HK, Breuer J, Lingens F, Hüttermann J, Kappl R, Fetzner S (1999) Eur J Biochem 263:871–878
48. Scholl HJ, Hüttermann J (1992) J Phys Chem 96:9684–9691
49. Sakaguchi U, Addison AW (1979) J Chem Soc Dalton Trans 4:600–608
50. Knecht S, Ricklin D, Eberle AN, Ernst B (2009) J Mol Recognit 22:270–279
51. Chen CW, Lin HL, Lin JC, Ho Y (2005) J Chin Chem Soc 52:1281–1290
52. Regan L (1993) Annu Rev Biophys Biomol Struct 22:257–281
53. Ullmann GM (2003) J Phys Chem B 107:1263–1271
54. Eftink MR, Ghiron C (1981) Anal Biochem 114:199–227
55. Lakowicz JR (1999) Principles of fluorescence spectroscopy, 2nd edn. Kluwer Academic, New York
56. Doose S, Neuweiler H, Sauer M (2009) ChemPhysChem 10:1389–1398
57. Murphy CJ, Arkin MR, Jenkins Y, Ghatlia ND, Bossmann SH, Turro, NJ, Barton JK (1993) Science 262:1025–1029
58. Schlag EW, Sheu SY, Yang DY, Selzle HL, Lin SH (2007) Angew Chem 119:3258–3273
59. Schlag EW, Sheu SY, Yang DY, Selzle HL, Lin SH (2007) Angew Chem Int Ed 46:3196–3199
60. Dietrich A, Buschmann V, Müller C, Sauer M (2002) Rev Mol Biotechnol 82:211–231
61. Edsall JT, Felsenfeld G, Goodman DS, Gurd FRN (1954) J Am Chem Soc 76:3054-3061
62. Förster T (1948) Ann Phys 2:55–75
63. Dale RE, Eisinger J, Blumberg WE (1979) Biophys J 26:161–194
64. Hitchman MA, Waite TD (1976) Inorg Chem 15:2150–2154
65. Selvin P.R, Hearst JE (1994) Proc Natl Acad Sci USA 91:10024–10028
66. Zimmer M (2002) Chem Rev 102:759–781
67. Khan YR, Dykstra TE, Scholes GD (2008) Chem Phys Lett 461:305–309
68. Sahoo H, Roccatano D, Hennig A, Nau WM (2007) J Am Chem Soc 129:9762–9772
69. Yang F, Moss LG, Phillips GN (1996) Nat Biotechnol 14:1246–1251